ROZPRAWY INŻYNIERSKIE • ENGINEERING TRANSACTIONS • 26, 3, 515—540, 1978
Polska Akademia Nauk • Instytut Podstawowych Problemów Techniki

CREEP RUPTURE OF STRUCTURES AT ELEVATED TEMPERATURE AND ESTIMATES OF RUPTURE LIFE

W. WOJEWÓDZKI (WARSZAWA)

A description of creep rupture at elevated temperature is proposed. The functions introduced to the constitutive equations were determined from the results of technically possible experiments in the uniaxial stress state. The description is shown to be useful in an investigation of the influence of the elevated temperature, the temperature gradients, its cyclic fluctuations and the cyclic proportional loading upon the stress redistribution, the amount of deformation, the propagation of the damage front and the rupture life of structures. Using the methods for bounding the rupture life of structures, the lower and upper bounds for simple structures were also obtained and compared with the given exact solution.

1. INTRODUCTION

The creep processes in metals are associated with physical mechanisms which, causing internal damage, weaken the material. As a result the stress redistribution occurs, the strain rate increases with time and a structure ruptures in the tertiary phase of creep. Elevated temperature accelerates the process of material deterioration. At low stress and high temperature a brittle type of fracture takes place (PENNY and MARRIOTT [1]). Many structural components, for example in nuclear reactors, operate in such loading conditions, hence this type of rupture will be considered.

Cyclic temperature and loading fluctuations may lead to an increase in the creep rate and shorten the time to rupture. The influence of cyclic fluctuations on creep depends on a number of factors: the material, the temperature and stress level, and the parameters of cycle, ODING et al [2], KENNEDY [3], TAIRA [4], TOFT and BROON [5], TILLY [6], and others.

Only a few creep data have been produced in which the stress is reversed periodically during the test. In the case of torsion the acceleration of the creep process was observed, NAMESTNIKOV [7], MORROW and HALFORD [8]. In the case of bending the test results have shown that for copper the material deterioration occurs only in tension and for aluminium under both tension and compression, HAYHURST [9].

Most experiments have been carried out under uni-axial stress states. The investigation of creep under variable loading and temperature conditions in the tri-axial stress states is a technically difficult problem and the available results have so far been insufficient.

The majority of existing theories accounting for variable loadings concern the primary and the secondary stages of creep and may be used in the special cases, [2],

RABOTNOV [10], PONTER [11], ODQVIST and HULT [12]. Long-term creep leading to rupture and accounting for the tertiary phase of creep may be considered from the stadpoint of accumulation of damage. This is recognized as KACHANOV's [13] concept of damage. Basing on this concept LECKIE and HAYHURST [14] suggested constitutive equations which reasonably represent the macroscopic behaviour of creeping material.

The aim of the present paper is to show, on the basis of these equations and the analysis of creep mechanisms, the possibilities of describing the creep rupture behaviour of a material at elevated constant and variable temperature and under constant or proportional cyclic loading. The influence of variable loading and the temperature gradient upon the rupture life and strains of a two-bar structure and a thick cylinder is investigated in detail. Also, the estimate of the rupture life of structures which are loaded at constant temperature is presented.

2. THE CONSTITUTIVE EQUATIONS

The total strain rate $\dot{\varepsilon}_{ij}$ is assumed to be the sum of the elastic $\dot{e}_{ij}$ and creep $\dot{v}_{ij}$ components, namely

$$\dot{\varepsilon}_{ij}=\dot{e}_{ij}+\dot{v}_{ij}. \tag{2.1}$$

The elastic strain e_{ij} is related to the stress σ_{ij} by

$$e_{ij}=C_{ijkl}\sigma_{kl}+\alpha\theta\delta_{ij}, \tag{2.2}$$

where C_{ijkr} is a tensor of elastic constants, α denotes the linear coefficient of thermal expansion and δ_{ij} is the Kronecker delta. The creep strain rate $\dot{v}_{ij}$ and the damage rate $\dot{\psi}$ can be described by the equations, LECKIE and HAYHURST [14],

$$\dot{v}_{ij}=\frac{K}{\psi^n}\varphi^n\frac{\partial\varphi}{\partial\sigma_{ij}}, \tag{2.3}$$

$$\dot{\psi}=-\frac{A}{\psi^v}A^v, \tag{2.4}$$

where the scalar functions φ and A are the homogeneous and convex functions of degree 1 in σ_{ij}. The functions φ and A are equal to σ when the applied stress is uniaxial. The material constants are represented by K, n, A, v. Basing on the studies reported by metal physicists, LECKIE and HAYHURST [14] suggested that the scalar function ψ can be used to measure the physical processes of deterioration. For undamaged material $\psi=1$, as damage occurs ψ decreases so that the strain rate increases. The rupture time t_r is obtained by integrating the relation (2.4) and applying the rupture condition $\psi=0$.

For a constant stress state, the expression for the rupture time is

$$t_r=1/[A\,(1+v)\,A^v]. \tag{2.5}$$

Isochronous surfaces are given by the condition $A\,(\sigma_{ij})=\text{const}$. The function $A\,(\sigma_{ij})$ can take various forms. Multi-axial rupture experiments show that the isochronous rupture surface of some important materials, such as stainless steel and aluminium alloys satisfy the Huber-Mises criterion of shear stress intensity. Other metals,

such as pure annealed copper and certain nimonic alloys, satisfy the maximum principal stress criterion. The rupture criterion for most metals apparently lies between these two extremes, SDOBYREV [15].

For variable uni-axial stresses the integration of the relation (2.4) gives the time-summation rupture condition

$$\Sigma (t/t_r) = 1 , \tag{2.6}$$

where t_r is the rupture time associated with the constant uni-axial stress σ_r. The extensive review by PENNY and MARRIOTT [1] of existing experimental data supports the view that the relation (2.6) is satisfactory for stepped cyclic loading of the type shown in Fig. 5 and, consequently, only proportional cyclic loading is considered.

For those materials whose isochronous surface $A(\sigma_{ij})$ is proportional to the constant energy-dissipation surface $\varphi(\sigma_{ij}) = \text{const}$, the constitutive relations are given by

$$\dot{v}_{ij} = \frac{K}{\psi^n} \varphi^n \frac{\partial \varphi}{\partial \sigma_{ij}} , \tag{2.7}$$

$$\dot{\psi} = -\frac{A}{\psi^v} \varphi^v , \tag{2.8}$$

For convenience, metals whose behaviour is described by Eqs. (2.7) and (2.8) are referred to as $\varphi - \varphi$ materials, while others whose behaviour is described by Eqs. (2.3) and (2.4) are referred to as $\varphi - A$ materials.

To account for the influence of elevated temperature and its changes on the creep process, the constants n, K, v, A, C_{ijkl} are assumed to be functions of temperature θ. Two functions K and A are introduced becouse the temperature dependence of creep and be failure may be different, these processes being characterized by different energies of activation. The creep strain rate and damage rate at any instant are determined by the actual stress state and temperature and depend on the structural state of the material which is characterized by ψ. The introduced functions n, K, v and A will be determined from the results of technically possible experiments in the uni-axial stress state which were carried out by GLEN and HAZRA [16] on steel specimens at loads from 2 to 28 T/in^2 and temperature from 450 to 575°C. Some results of these tests are presented in Fig. 1, 2, 3; more information may be found in Ref. WOJEWÓDZKI [17]. Integration of Eqs. (2.7) and (2.8) for the uni-axial stress state in which $\sigma = \text{const}$ and $\theta = \text{const}$ yields

$$v = K\sigma^n \frac{t_r}{1 - n/(1+v)} \left[1 - \left(1 - \frac{t}{t_r} \right)^{1 - n/(1+v)} \right] , \tag{2.9}$$

$$\psi = \left(1 - \frac{t}{t_r} \right)^{1/(1+v)} , \tag{2.10}$$

$$t_r = 1/[(1+v) A \sigma^v] . \tag{2.11}$$

For $t = t_r$ we have $v = (K/A)\, \sigma^{n-v}/(1+v-n)$, where $1+v > n \geqslant v$. If this restriction cannot be satisfied for some materials it is possible to introduce more parameters into the constitutive equations, see [10]. The expression (2.11) gives a linear relationship between $\log \sigma$ and $\log t_r$ observed experimentally over a considerable stress

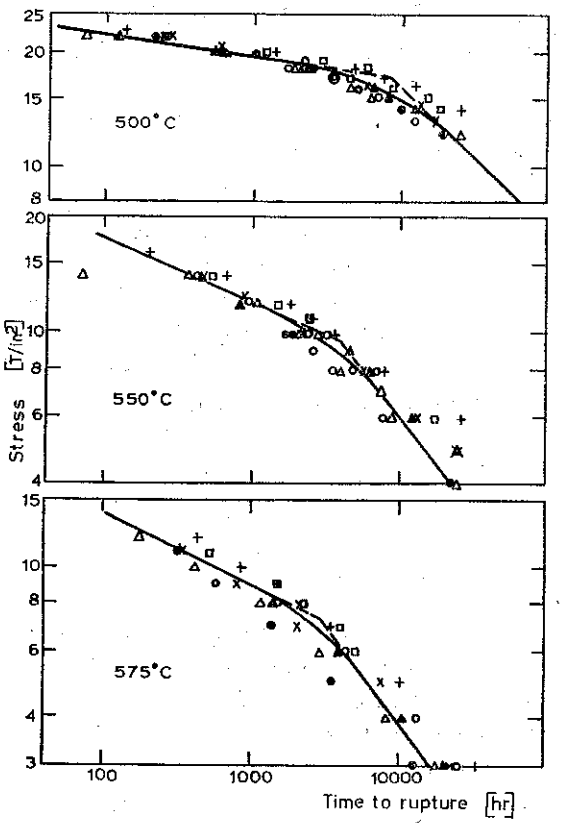

FIG. 1. Uni-axial stress-time to rupture data for BS 1501–271 steel.

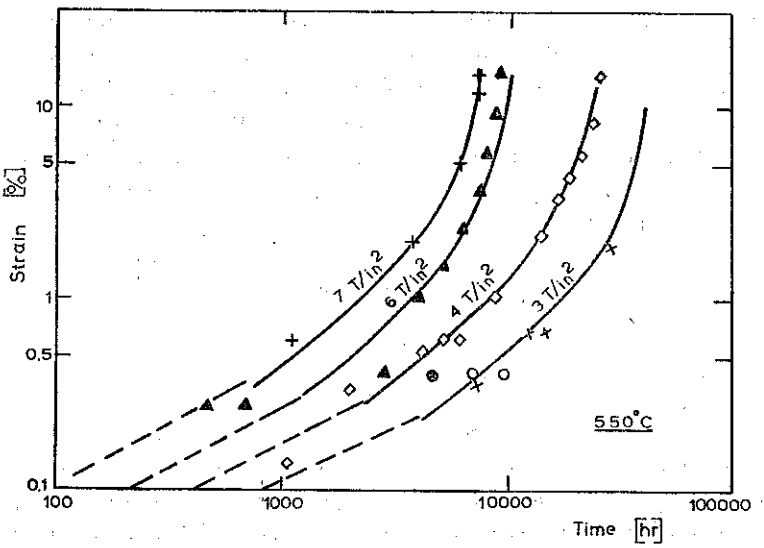

FIG. 2. Creep curves to rupture for BS 1501–271 steel.

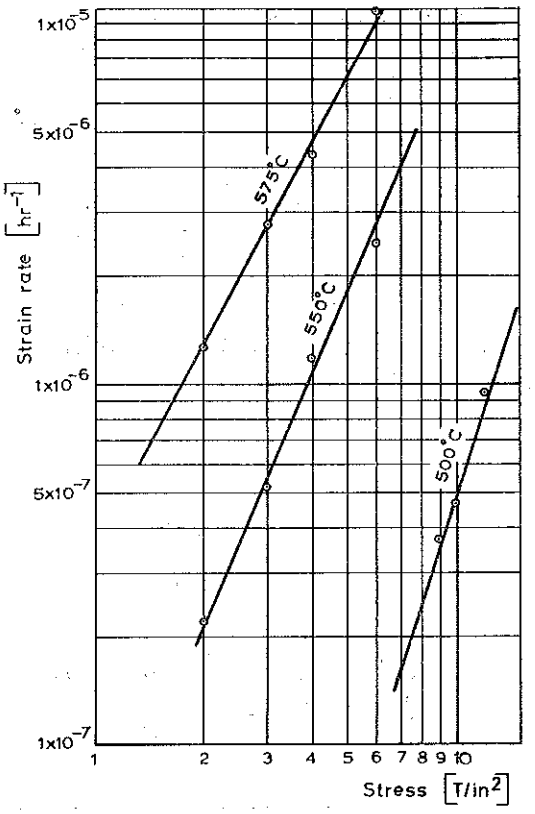

FIG. 3. Relationship between stress and creep rate in the steady state conditions for BS 1501–271 steel

range, Fig. 1, and therefore from this rupture curve the values of v and A can be obtained. Similarly, in the steady state creep condition, from a linear relation between $\log v$ and $\log \sigma$, Fig. 3, the values of n and K can be calculated. The determined functions n, K, v and A in the temperature range 500–575°C and for lower stress level have the following form:

$$n = -1.333 \cdot 10^{-5}\,\theta^2 - 3 \cdot 10^{-3}\,\theta + 8.033, \tag{2.12}$$

$$K = \exp\left[-37.9561032 + 47.003878 \cdot 10^3 \left(\frac{1}{500} - \frac{1}{\theta}\right) + 17.5180052 \cdot 10^6 \left(\frac{1}{500} - \frac{1}{\theta}\right)^2\right], \tag{2.13}$$

$$v = 12.267 \cdot 10^{-5}\,\theta^2 - 143.200 \cdot 10^{-3}\,\theta + 43.6133, \tag{2.14}$$

$$A = \exp\left[-31.4431988 + 57.478940 \cdot 10^3 \left(\frac{1}{500} - \frac{1}{\theta}\right) - 80.2612757 \cdot 10^6 \left(\frac{1}{500} - \frac{1}{\theta}\right)^2\right]. \tag{2.15}$$

Table 1. Values of functions n, K, ν and A

θ [°C]	n	K $\left[\left(\frac{\text{KG}}{\text{cm}^2}\right)^{-n} hr^{-1}\right]$	ν	A $\left[\left(\frac{\text{KG}}{\text{cm}^2}\right)^{-\nu} hr^{-1}\right]$
500	3.2	$3.28 \cdot 10^{-17}$	2.68	$2.21 \cdot 10^{-14}$
525	2.784	$3.38085 \cdot 10^{-15}$	2.2443	$2.5447 \cdot 10^{-12}$
550	2.35	$3.0125 \cdot 10^{-13}$	1.96	$5.38 \cdot 10^{-11}$
575	1.90	$2.285 \cdot 10^{-11}$	1.83	$3.05 \cdot 10^{-10}$

Table 2. The calculated values of rupture time for the specimens and the corresponding strains

σ $\left[\frac{\text{KG}}{\text{cm}^2}\right]$, $\left[\frac{\text{T}}{\text{in}^2}\right]$		500°C		550°C		575°C	
		t_r [hr]	v [%]	t_r [hr]	v [%]	t_r [hr]	v [%]
310	2			81300	8.47	32000	12.70
465	3			37000	9.84	15600	12.95
620	4	415000	9.001	22180	12.03	9190	13.10
930	6	139000	11.035	10000	13.52	4340	13.76
1085	7			7022	13.90		
1240	8	61200	12.198	5404	14.63		
1395	9	45950	13.35				
1550	10	34574	14.074	3500			
1860	12	21210	15.473				
2170	14	14061	16.80				

The values and dimensions of these functions for four levels of temperature are given in Table 1. The values of the rupture times calculated from Eqs. (2.11) and (2.9) and the corresponding rupture strains for the investigated specimens are presented in Table 2. Also, the creep curves obtained from Eq. (2.9) are shown in Fig. 2 by a solid line. The broken lines represent the steady state creep. Equation (2.9) takes no account of primary creep.Fairly good agreement with experiments can be seen in the investigated range of stress and temperature.

3. Examples of analysis of the structures

3.1. Two-bar structure

The structure shown in Fig. 4 enables to realize a desirable stress concentration factor and to estimate the description of creep rupture behaviour of a structure under variable temperature and loading conditions. The following cases of loading will be considered, Fig. 5:

a) constant load ($\lambda=1$) and temperature ($\Delta\theta=\theta$),
b) constant load ($\lambda=1$) and cyclic temperature,
c) cyclic load and constant temperature ($\Delta\theta=0$),
d) cyclic load and temperature.

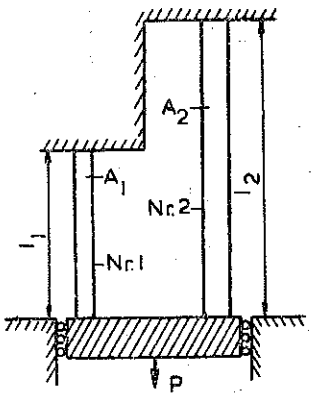

FIG. 4. Two-bar structure.

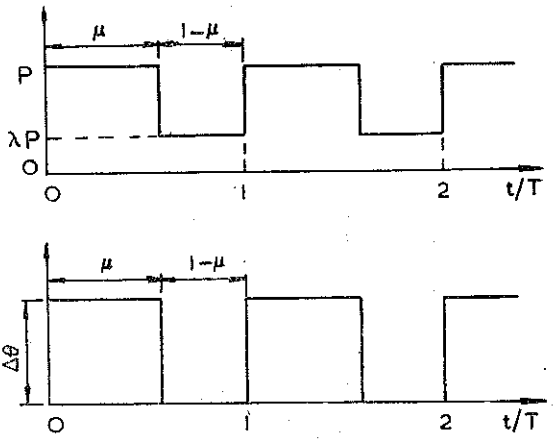

FIG. 5. Cyclic loading and cyclic temperature variations

In this situation the equations of equilibrium, compatibility and the constitutive equations have the form

$$\gamma_1 \sigma_1 + \sigma_2 = \begin{cases} p & \text{for} \quad 0 \leqslant t \leqslant \mu T, \\ \lambda p & \text{for} \quad \mu T \leqslant t \leqslant T, \end{cases} \tag{3.1}$$

$$\frac{\dot{\sigma}_1}{E} + K\left(\frac{|\sigma_1|}{\psi_1}\right)^n \operatorname{sgn}\sigma_1 = \beta_1\left[\frac{\dot{\sigma}_2}{E} + K\left(\frac{|\sigma_2|}{\psi_2}\right)^n \operatorname{sgn}\sigma_2\right], \tag{3.2}$$

$$\dot{\psi}_i = -A\left(\frac{|\sigma_i|}{\psi_i}\right)^\nu, \qquad i=1,\ 2, \tag{3.3}$$

$$\varepsilon_i = \frac{\sigma_i}{E} + \alpha\Delta\theta + \int_0^t K\left(\frac{|\sigma_i|}{\psi_i}\right)^n \operatorname{sgn}\sigma_i \, dt, \qquad i=1,\ 2, \tag{3.4}$$

where $\gamma_1 = A_1/A_2$, $\beta_1 = l_2/l_1$, $p = P/A_2$, E—modulus of elasticity. The values of n, K, ν and A are given by Eqs. (2.12)–(2.15). It is assumed that the material is of the $\varphi - \varphi$ type and material damage occurs equally under tension and compression. The initial conditions at the instant $t=0$ are determined by $\psi_i = 1$ and the behaviour of elastic structure,

$$\sigma_1 = \frac{\beta_1 p + E(\beta_1 - 1)\,\alpha\Delta\theta}{1+\gamma_1\beta_1}, \qquad \sigma_2 = \frac{p - \gamma_1 E(\beta - 1)\,\alpha\Delta\theta}{1+\gamma_1\beta_1}. \tag{3.5}$$

Equations (3.1) and (3.2) are valid until the first bar ruptures. After this instant of time t_{r1} the structure became statically determinate but was able to sustain load until the time t_{r2} when the second bar ruptured. The equations were integrated numerically for the following values: $p = 620$ kG/cm^2, $\beta_1 = 0.5$, $\beta_1 = 2°$, $\lambda = \mu = 0.5$, $T = 24$ hrs, $\alpha = 1 \cdot 10^{-5}$ 1/°C, $E = 1.5 \cdot 10^6$ kG/cm^2. Linear influence of temperature on the modulus E was accounted for, taking the value for 500°C. Variable steps of

Table 3. Two-bar structures. Rupture times and corresponding strains

P=const. θ=const.		P=const. θ=cycl.		P=cycl. θ=const.		P=cycl. θ=cycl.	
1st Bar	2nd Bar	1st Bar	2nd Bar	1st Bar	2nd Bar	1st Bar	2nd Bar
500°C		500–550°C		500°C		500–550°C	
t_r=111.804·10⁴	113.912·10⁴	8.028·10⁴	8.41785·10⁴	188.837·10⁴	191.3615·10⁴	7.9572·10⁴	8.62803·10⁴
N=46585	47464	3345	3508	78683	79734	3316	3596
ε=4.862	8.057	8.64	10.00	4.254	7.8	7.04	10.60
550°C		550–575°C		550°C			
t_r=4.30461·10⁴	4.49547·10⁴	2.43221·10⁴	2.55303·10⁴	6.7512·10⁴	7.07135·10⁴		
N=1794	1874	1014	1064	2814	2947		
ε=7.825	10.80	11.37	12.372	7.167	10.181		
575°C		500–575°C		575°C		500–575°C	
t_r=1.68384·10⁴	1.80360·10⁴	3.1872·10⁴	3.46412·10⁴	2.568·10⁴	2.784·10⁴	3.09223·10⁴	3.48171·10⁴
N=702	752	1328	1444	1070	1160	1289	1451
ε=12.02	12.207	10.905	12.223	11.278	12.385	9.737	12.934

$p=\frac{P}{A_2}$=620 KG/cm², $\mu=\lambda$=0.5, T=24 hrs, β_1=2, γ_1=0.5, t_r—[hr], ε—[%], N—Number of days or cycles

calculations were adopted and after each step of time the equations of equilibrium and compatibility were checked. The numerical results are given in Table 3. Also, in Fig. 6, the creep strains over a day or cycle are presented.

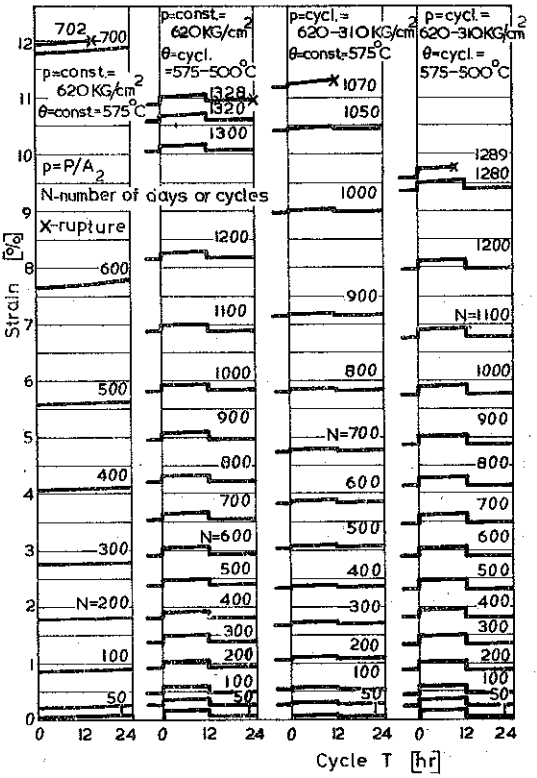

FIG. 6. Cyclic strains of the bar No 1.

3.2. Thick cylinder

We shall consider the axisymmetric problem of an infinitely long thick cylinder subjected to internal constant or proportional cyclic pressure and to a constant or cyclic temperature gradient, Figs. 7 and 5. In this situation we have the following relationships:

$$\frac{\partial \sigma_r}{\partial r} + \frac{\sigma_r - \sigma_\varphi}{r} = 0, \tag{3.6}$$

$$\dot{v}_r = \frac{\partial \dot{u}}{\partial r}, \qquad \dot{v}_\varphi = \frac{\dot{u}}{r}. \tag{3.7}$$

From the equation $\dot{v}_r + \dot{v}_\varphi = 0$ ($\dot{v}_z = 0$, the plane strain conditions) we get an outward radial velocity

$$\dot{u} = C(t)/r. \tag{3.8}$$

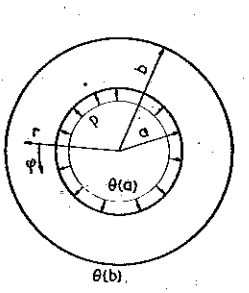

FIG. 7. Thick cylinders; coordinates, dimensions and loading.

Assuming $\varphi=\sigma_\varphi-\sigma_r$ and using Eqs. (2.7), (2.8), (3.6) and (3.8), we obtain the basic set of equations (elastic strains are neglected):

$$\frac{1}{\psi}\frac{\partial\sigma_r}{\partial r}=\frac{C(t)^{1/n}}{K^{1/n}r^{2/n+1}}, \tag{3.9}$$

$$\sigma_\varphi=\frac{\partial(r\sigma_r)}{\partial r}, \tag{3.10}$$

$$\sigma_z=\frac{1}{2}(\sigma_r+\sigma_\varphi), \tag{3.11}$$

$$\dot{\psi}=-A\left(\frac{C(t)}{Kr^2}\right)^{\nu/n}. \tag{3.12}$$

We will consider the steady heat flow described by the equation

$$\theta(r)=\theta(a)+\frac{\theta(b)-\theta(a)}{\ln(b/a)}\ln(r/a), \tag{3.13}$$

where $\theta(a)$, $\theta(b)$ are the temperatures of the internal and external surfaces of the tube, respectively. Thus the values of n, K, ν and A at any radius are determined by Eqs. (2.12)–(2.15) and (3.13). This set of equations can be only integrated numerically with the use of a computer. Two constants are determined by two boundary conditions.

The strains and radial displacement are given by

$$v_r=-v_\varphi, \qquad v_\varphi=\int_0^t\frac{C(t)}{r^2}dt, \qquad u=\int_0^t\frac{C(t)}{r}dt. \tag{3.14}$$

It can be seen from Eq. (3.12), for a constant temperature ($\Delta\theta=0$), that ψ will become zero first at the inner boundary, $r=a$. Let us introduce a new floating boundary at $r=s$, so that $\psi=0$ for $r\leqslant s$. In a general case where the temperature gradient exists, ψ may become zero first for the arbitrary value of $a\leqslant r\leqslant b$. It depends, for a given geometry of tube, on the value of pressure, temperature gradient and its direction. In such cases the integration will be terminated at the instant when $\psi=0$, while for the situation where ψ becomes zero first at $r=a$, the integration will be carried out in full. For a cylinder made of the $\varphi-\varphi$ material the stress σ_φ may take negative values in the regions near the inner boundary at the time just before the the first rupture and before the next ruptures. These values of σ_φ are, in general, smaller than σ_r, so the basic set of equations was assumed to remain valid in such situations.

For convenience we introduce the following quantities:

$$\xi=r/a, \qquad \zeta=s/a, \qquad h=b/a, \qquad c(t)=C(t)/a^2. \tag{3.15}$$

The basic Eqs. (3.9)–(3.14) then become

$$\frac{1}{\psi}\frac{\partial\sigma_r}{\partial\xi}=\left(\frac{c}{K}\right)^{1/n}\frac{1}{\xi^{2/n+1}}, \tag{3.16}$$

$$\sigma_\varphi = \frac{\partial(\xi\sigma_r)}{\partial\xi}, \tag{3.17}$$

$$\sigma_z = \frac{1}{2}(\sigma_r + \sigma_\varphi), \tag{3.18}$$

$$\dot{\psi} = -A\left(\frac{c}{K\xi^2}\right)^{\nu/n}, \tag{3.19}$$

$$\theta(\xi) = \theta(1) + \frac{\theta(h)-\theta(1)}{\ln h}\ln\xi, \quad \text{when } \psi>0 \quad \text{everywhere}, \tag{3.20}$$

$$\theta(\xi) = \theta(1) + \frac{\theta(h)-\theta(1)}{\ln(h/\zeta)}\ln(\xi/\zeta). \quad \text{when } \psi=0 \quad \text{for} \quad \xi\leqslant\zeta, \tag{3.21}$$

$$v_r = -v_\varphi, \qquad v_\varphi = \int_0^t \frac{c}{\xi^2}\,dt, \qquad u = a\int_0^t \frac{c}{\xi}\,dt, \tag{3.22}$$

The boundary conditions then are

$$\sigma_r(1) = \begin{cases} -P & \text{for } 0\leqslant t\leqslant \mu T, \\ -\lambda P & \text{for } \mu T\leqslant t\leqslant T, \end{cases} \qquad \sigma_r(h)=0 \quad \text{when } \psi>0 \text{ everywhere}, \tag{3.23}$$

$$\sigma_r(\zeta) = \begin{cases} -P & \text{for } 0\leqslant t\leqslant \mu T, \\ -\lambda P & \text{for } \mu T\leqslant t\leqslant T, \end{cases} \qquad \sigma_r(h)=0 \quad \text{when } \psi=0 \quad \text{for } \xi\leqslant\zeta. \tag{3.24}$$

The problem was solved numerically by means of a CDC computer for the following values: $P=310$ kG/cm^2, $\lambda=0.4$, $\mu=2/3$, $T=24$ hours, $h=1.5$ and for the temperature range 500–575°C. The step of time was taken equal to 2 hours and the thickness

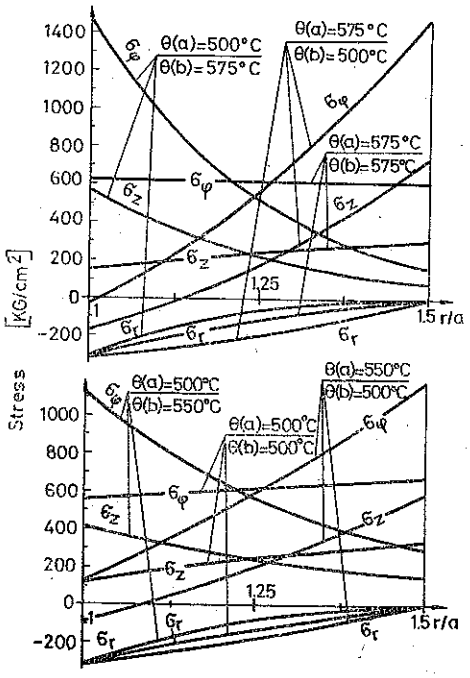

FIG. 8. Stress distribution in the steady state creep conditions in a thick cylinder for different temperature gradients

Assuming $\varphi=\sigma_\varphi-\sigma_r$ and using Eqs. (2.7), (2.8), (3.6) and (3.8), we obtain the basic set of equations (elastic strains are neglected):

$$\frac{1}{\psi}\frac{\partial\sigma_r}{\partial r}=\frac{C(t)^{1/n}}{K^{1/n}r^{2/n+1}}, \tag{3.9}$$

$$\sigma_\varphi=\frac{\partial(r\sigma_r)}{\partial r}, \tag{3.10}$$

$$\sigma_z=\frac{1}{2}(\sigma_r+\sigma_\varphi), \tag{3.11}$$

$$\dot{\psi}=-A\left(\frac{C(t)}{Kr^2}\right)^{\nu/n}. \tag{3.12}$$

We will consider the steady heat flow described by the equation

$$\theta(r)=\theta(a)+\frac{\theta(b)-\theta(a)}{\ln(b/a)}\ln(r/a), \tag{3.13}$$

where $\theta(a)$, $\theta(b)$ are the temperatures of the internal and external surfaces of the tube, respectively. Thus the values of n, K, ν and A at any radius are determined by Eqs. (2.12)–(2.15) and (3.13). This set of equations can be only integrated numerically with the use of a computer. Two constants are determined by two boundary conditions.

The strains and radial displacement are given by

$$v_r=-v_\varphi, \qquad v_\varphi=\int_0^t\frac{C(t)}{r^2}dt, \qquad u=\int_0^t\frac{C(t)}{r}dt. \tag{3.14}$$

It can be seen from Eq. (3.12), for a constant temperature ($\Delta\theta=0$), that ψ will become zero first at the inner boundary, $r=a$. Let us introduce a new floating boundary at $r=s$, so that $\psi=0$ for $r\leqslant s$. In a general case where the temperature gradient exists, ψ may become zero first for the arbitrary value of $a\leqslant r\leqslant b$. It depends, for a given geometry of tube, on the value of pressure, temperature gradient and its direction. In such cases the integration will be terminated at the instant when $\psi=0$, while for the situation where ψ becomes zero first at $r=a$, the integration will be carried out in full. For a cylinder made of the $\varphi-\varphi$ material the stress σ_φ may take negative values in the regions near the inner boundary at the time just before the the first rupture and before the next ruptures. These values of σ_φ are, in general, smaller than σ_r, so the basic set of equations was assumed to remain valid in such situations.

For convenience we introduce the following quantities:

$$\xi=r/a, \qquad \zeta=s/a, \qquad h=b/a, \qquad c(t)=C(t)/a^2. \tag{3.15}$$

The basic Eqs. (3.9)–(3.14) then become

$$\frac{1}{\psi}\frac{\partial\sigma_r}{\partial\xi}=\left(\frac{c}{K}\right)^{1/n}\frac{1}{\xi^{2/n+1}}, \tag{3.16}$$

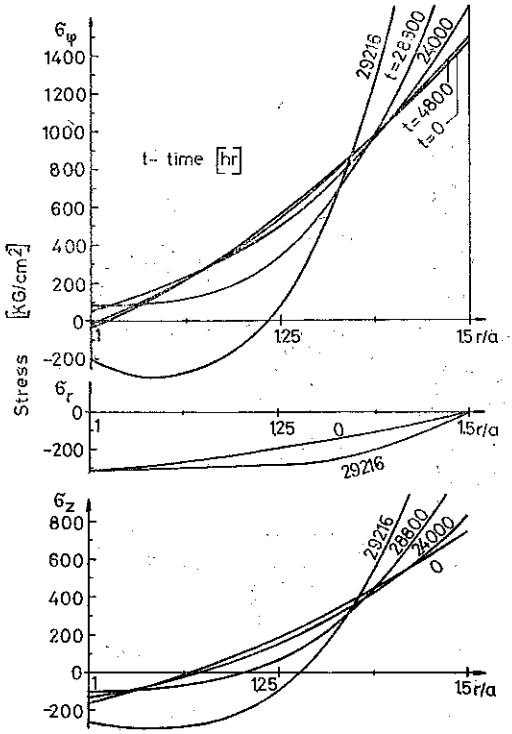

FIG. 11. Stress redistribution in a thick cylinder for constant pressure and the constant temperature gradient $\theta\,(a)=575°C$, $\theta\,(b)=500°C$.

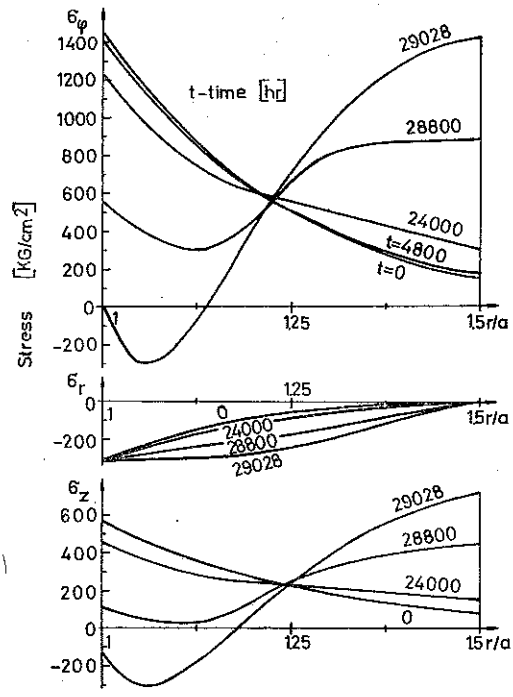

FIG. 12. Stress redistribution in a thick cylinder for constant pressure and the constant temperature gradient $\theta\,(a)=500°C$, $\theta\,(b)=575°C$.

$$\sigma_\varphi = \frac{\partial(\xi\sigma_r)}{\partial\xi}, \tag{3.17}$$

$$\sigma_z = \frac{1}{2}(\sigma_r + \sigma_\varphi), \tag{3.18}$$

$$\dot{\psi} = -A\left(\frac{c}{K\xi^2}\right)^{n/n}, \tag{3.19}$$

$$\theta(\xi) = \theta(1) + \frac{\theta(h)-\theta(1)}{\ln h}\ln\xi, \quad \text{when } \psi > 0 \quad \text{everywhere}, \tag{3.20}$$

$$\theta(\xi) = \theta(1) + \frac{\theta(h)-\theta(1)}{\ln(h/\zeta)}\ln(\xi/\zeta). \quad \text{when } \psi = 0 \quad \text{for} \quad \xi \leqslant \zeta, \tag{3.21}$$

$$v_r = -v_\varphi, \qquad v_\varphi = \int_0^t \frac{c}{\xi^2}\,dt, \qquad u = a\int_0^t \frac{c}{\xi}\,dt, \tag{3.22}$$

The boundary conditions then are

$$\sigma_r(1) = \begin{cases} -P & \text{for } 0 \leqslant t \leqslant \mu T, \\ -\lambda P & \text{for } \mu T \leqslant t \leqslant T, \end{cases} \quad \sigma_r(h) = 0 \quad \text{when } \psi > 0 \text{ everywhere}, \tag{3.23}$$

$$\sigma_r(\zeta) = \begin{cases} -P & \text{for } 0 \leqslant t \leqslant \mu T, \\ -\lambda P & \text{for } \mu T \leqslant t \leqslant T, \end{cases} \quad \sigma_r(h) = 0 \quad \text{when } \psi = 0 \quad \text{for } \xi \leqslant \zeta. \tag{3.24}$$

The problem was solved numerically by means of a CDC computer for the following values: $P = 310$ kG/cm^2, $\lambda = 0.4$, $\mu = 2/3$, $T = 24$ hours, $h = 1.5$ and for the temperature range 500–575°C. The step of time was taken equal to 2 hours and the thickness

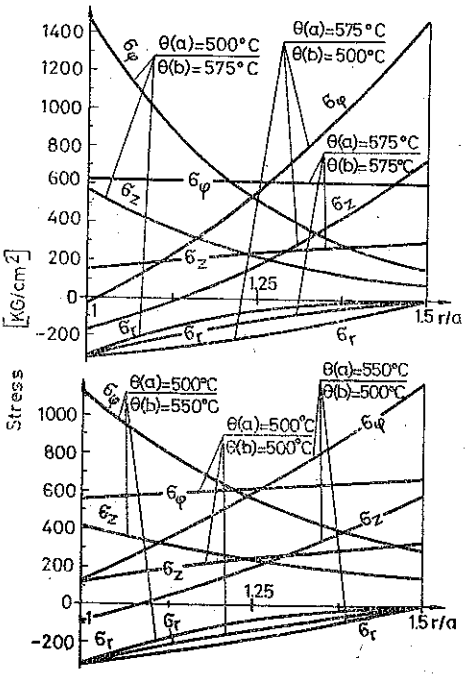

FIG. 8. Stress distribution in the steady state creep conditions in a thick cylinder for different temperature gradients

The upper bounds are:

for a constant load (P_i=const.)

$$t_u = V \Big/ \Big[A(1+\nu) \int_V \Delta^\nu(\bar{\sigma}^s_{ij})\, dV \Big], \tag{4.1}$$

for cyclic loading $(P_i\, \gamma(t)$, where $\gamma(t)=\gamma(t+T))$

$$t_u = V \Big/ \Big[A(1+\nu) \int_0^1 \gamma^\nu(x)\, dx \int_V \Delta^\nu(\bar{\sigma}^t_{ij})\, dV \Big], \tag{4.2}$$

where $t=xT$, T is the length of cycle, V—denotes the volume of a component, $\bar{\sigma}^s_{ij}$ is the steady state solution for a hypothetical body identical in shape to that under consideration and subjected to traction P_i. The material of this body is an elastic creeping material with the constitutive relations

$$e_{ij} = C_{ijkl}\, \sigma_{kl}, \qquad \dot{v}_{ij} = K \Delta^{\nu-1}\, \partial \Delta / \partial \sigma_{ij}. \tag{4.3}$$

This material does not suffer material deterioration. The results in Eqs. (4.1) and (4.2) may be expressed in terms of representative rupture stresses which give the time to rupture for a uni-axial specimen equal to the time to rupture for the structural component. Thus the structural performance can readily be related to the material behaviour. For a constant load, the representative rupture stress is σ_u and for cyclic loading, $\sigma_u\, \gamma(t)$ where

$$\sigma_u = \Big[\int_V \Delta^\nu(\bar{\sigma}^s_{ij})\, dV/V \Big]^{1/\nu}. \tag{4.4}$$

In the case of the $\varphi - \varphi$ material the symbol Δ in Eqs. (4.1)–(4.4.) should be replaced by φ.

The lower bounds are not of such generality as the upper bounds. They are limited to kinematically determinate structural components. However, LECKIE and HAYHURST [14] have shown experimentally that these bounds satisfactorily predict the life of the structure which are not strictly kinematically determinate and subjected to a constant load. The lower bounds for $\varphi - \varphi$ material are:

for constant load (LECKIE and HAYHURST [14])

$$t_l = \int_V \varphi^{n+1}(\sigma^s_{ij})\, dV \Big/ \Big[A(1+\nu) \int_V \varphi^{n+1+\nu}(\sigma^s_{ij})\, dV \Big], \tag{4.5}$$

where σ^s_{ij} is the steady state stress distribution:

for cyclic loading

$$t_l = \int_V \bar{\varphi} dV \Big/ \Big[A(1+\nu) \int_V \bar{\varphi} \int_0^1 \varphi^\nu(\sigma^{sc}_{ij})\, dx dV \Big], \tag{4.6}$$

where $\bar{\varphi} = \int_0^1 \varphi^{n+1}(\sigma^{sc}_{ij})\, dx$, σ^{sc}_{ij} is the steady-state cyclic stress distribution. In situations where the cycle time T is small in relation to the working life of the structure, $\sigma^{sc}_{ij} = \sigma^e_{ij} + \rho_{ij}$, where σ^d_{ij} is the elastic stress distribution in equilibrium with the cyclic

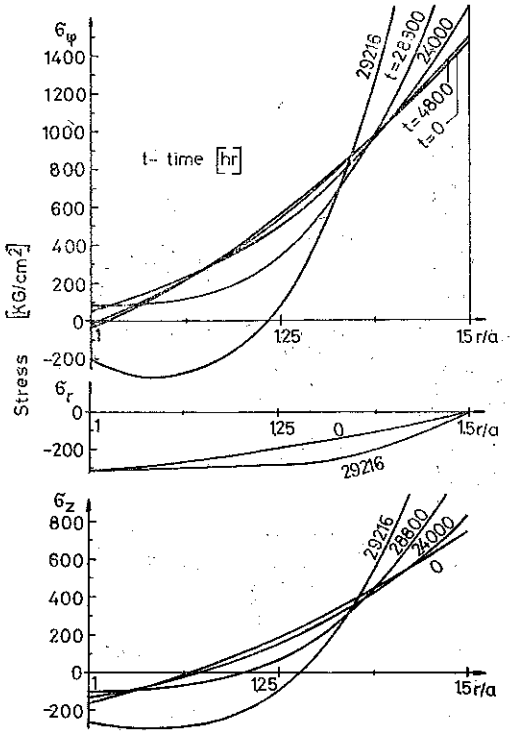

FIG. 11. Stress redistribution in a thick cylinder for constant pressure and the constant temperature gradient $\theta\,(a)=575°C$, $\theta\,(b)=500°C$.

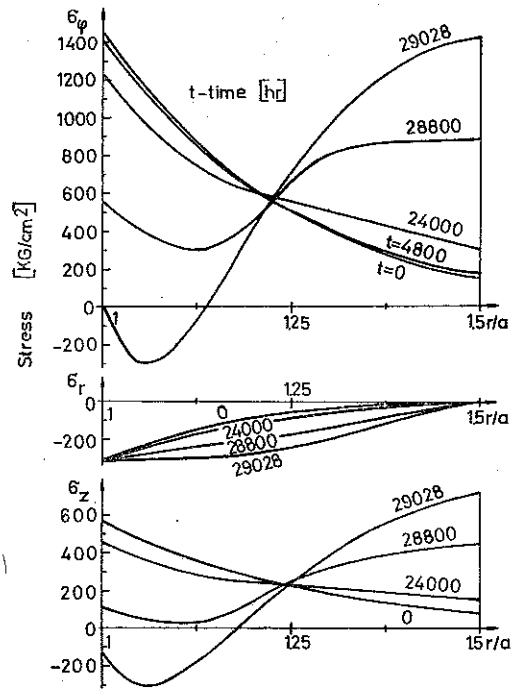

FIG. 12. Stress redistribution in a thick cylinder for constant pressure and the constant temperature gradient $\theta\,(a)=500°C$, $\theta\,(b)=575°C$.

The corresponding representative rupture stresses are: for a constant load, σ_u, for cyclic loading, $\sigma_u\,\gamma\,(t)$, where

$$\frac{\sigma_u}{p}=1/[(\gamma_1/\beta_1+1)\,(\gamma_1\,\beta_1^{1/(\nu-1)}+1)^{\nu-1}]^{1/\nu}. \tag{4.15}$$

Now, the lower bounds on rupture life will be given. Finding the steady state distribution σ_{ij}^s and inserting it into Eqs. (4.5) and (4.7), we obtain for the case of a constant load the following expressions for the lower bound on rupture time and the representative rupture stress:

$$t=\frac{(\gamma_1\,\beta_1^{1/n}+1)^{\nu+1}}{(1+\nu)\,Ap^{\nu}(\gamma_1\,\beta_1^{(\nu+1)/n}+1)}, \tag{4.16}$$

$$\frac{\sigma_l}{p}=\frac{(\gamma_1\,\beta_1^{(\nu+1)/n}+1)^{1/\nu}}{(\gamma_1\,\beta_1^{1/n}+1)^{(\nu+1)/\nu}}. \tag{4.17}$$

For the case of cylic loading it is necessary to know the cyclic steady-state stress distribution $\sigma_{ij}^{sc}(t)=\sigma_{ij}^e(t)+\rho_{ij}$. This state is found by choosing ρ to minimize the expression for the energy dissipation D over a cycle

$$\frac{D}{TA_2\,l_2\,p^{n+1}}=\mu\left[\frac{\gamma_1}{\beta_1}\left(\frac{\beta_1}{\gamma_1\,\beta_1+1}-\rho\right)^{n+1}+\left(\frac{1}{\gamma_1\,\beta_1+1}+\frac{\rho}{2}\right)^{n+1}\right]+ \tag{4.18}$$

$$+(1-\mu)\left[\frac{\gamma_1}{\beta_1}\left(\frac{\beta_1\,\lambda}{\gamma_1\,\beta_1+1}-\rho\right)^{n+1}+\left(\frac{\lambda}{\gamma_1\,\beta_1+1}+\frac{\rho}{2}\right)^{n+1}\right],$$

where $\rho=-\rho_1/p$ is a measure of the self-equilibrating stress field. On using this minimum value ρ and the expression (4.6), we arrive at the formula for the rupture time

$$t_l=\frac{\mu\left[\left(\frac{\beta_1}{\gamma_1\,\beta_1+1}-\rho\right)^{n+1}+\frac{\beta_1}{\gamma_1}\left(\frac{1}{\gamma_1\,\beta_1+1}+\frac{\rho}{2}\right)^{n+1}\right]+}{+(1-\mu)\left[\left(\frac{\lambda\beta_1}{\gamma_1\,\beta_1+1}-\rho\right)^{n+1}+\frac{\beta_1}{\gamma_1}\left(\frac{\lambda}{\gamma_1\,\beta_1+1}+\frac{\rho}{2}\right)^{n+1}\right]} \tag{4.19}$$

$$(1+\nu)\,Ap^{\nu}\left\{\mu\left[\left(\frac{\beta_1}{\gamma_1\,\beta_1+1}-\rho\right)^{n+1+\nu}+\frac{\beta_1}{\gamma_1}\left(\frac{1}{\gamma_1\,\beta_1+1}+\frac{\rho}{2}\right)^{n+1+\nu}\right]+\right.$$

$$\left.+(1-\mu)\left[\left(\frac{\lambda\beta_1}{\gamma_1\,\beta_1+1}-\rho\right)^{n+1+\nu}+\frac{\beta_1}{\gamma_1}\left(\frac{\lambda}{\gamma_1\,\beta_1+1}+\frac{\rho}{2}\right)^{n+1+\nu}\right]\right\}.$$

The corresponding representative rupture stress is $\sigma_l\,\gamma\,(t)$, where

$$\frac{\sigma_l}{p}=1/\{(1+\nu)\,Ap^{\nu}\,t_l\,[\mu+\lambda^{\nu}(1-\mu)]\}^{1/\nu}. \tag{4.20}$$

The above expressions are valid for the two-bar structure which operates at constant temperature. Data for the computations are given in Sect. 3.1 and the numerical results are presented in Table 5. It was found that the values $\rho=0.214$; 0.170; 0.135 minimized the energy dissipation, Eq. (4.18), for $\theta=500$; 550; 575°C, respectively.

The upper bounds are:

for a constant load (P_i=const.)

$$t_u = V \Big/ \Big[A(1+\nu) \int_V \Delta^\nu(\bar{\sigma}^s_{ij})\, dV \Big], \tag{4.1}$$

for cyclic loading $(P_i\, \gamma(t)$, where $\gamma(t)=\gamma(t+T))$

$$t_u = V \Big/ \Big[A(1+\nu) \int_0^1 \gamma^\nu(x)\, dx \int_V \Delta^\nu(\bar{\sigma}^t_{ij})\, dV \Big], \tag{4.2}$$

where $t=xT$, T is the length of cycle, V—denotes the volume of a component, $\bar{\sigma}^s_{ij}$ is the steady state solution for a hypothetical body identical in shape to that under consideration and subjected to traction P_i. The material of this body is an elastic creeping material with the constitutive relations

$$e_{ij} = C_{ijkl}\, \sigma_{kl}, \qquad \dot{v}_{ij} = K \Delta^{\nu-1}\, \partial \Delta / \partial \sigma_{ij}. \tag{4.3}$$

This material does not suffer material deterioration. The results in Eqs. (4.1) and (4.2) may be expressed in terms of representative rupture stresses which give the time to rupture for a uni-axial specimen equal to the time to rupture for the structural component. Thus the structural performance can readily be related to the material behaviour. For a constant load, the representative rupture stress is σ_u and for cyclic loading, $\sigma_u\, \gamma(t)$ where

$$\sigma_u = \Big[\int_V \Delta^\nu(\bar{\sigma}^s_{ij})\, dV/V \Big]^{1/\nu}. \tag{4.4}$$

In the case of the $\varphi - \varphi$ material the symbol Δ in Eqs. (4.1)–(4.4.) should be replaced by φ.

The lower bounds are not of such generality as the upper bounds. They are limited to kinematically determinate structural components. However, LECKIE and HAYHURST [14] have shown experimentally that these bounds satisfactorily predict the life of the structure which are not strictly kinematically determinate and subjected to a constant load. The lower bounds for $\varphi - \varphi$ material are:

for constant load (LECKIE and HAYHURST [14])

$$t_l = \int_V \varphi^{n+1}(\sigma^s_{ij})\, dV \Big/ \Big[A(1+\nu) \int_V \varphi^{n+1+\nu}(\sigma^s_{ij})\, dV \Big], \tag{4.5}$$

where σ^s_{ij} is the steady state stress distribution:

for cyclic loading

$$t_l = \int_V \bar{\varphi} dV \Big/ \Big[A(1+\nu) \int_V \bar{\varphi} \int_0^1 \varphi^\nu(\sigma^{sc}_{ij})\, dx dV \Big], \tag{4.6}$$

where $\bar{\varphi} = \int_0^1 \varphi^{n+1}(\sigma^{sc}_{ij})\, dx$, σ^{sc}_{ij} is the steady-state cyclic stress distribution. In situations where the cycle time T is small in relation to the working life of the structure, $\sigma^{sc}_{ij} = \sigma^e_{ij} + \rho_{ij}$, where σ^d_{ij} is the elastic stress distribution in equilibrium with the cyclic

and the representative rupture stress σ_u for a constant load and $\sigma_u\,\gamma(t)$ for a cyclic load,

$$\frac{\sigma_u}{P}=2\left\{\left[(\nu-1)\left(1-\left(\frac{a}{b}\right)^{2/(\nu-1)}\right)\right]^{1-\nu}\Big/\left(\left(\frac{b}{a}\right)^2-1\right)\right\}^{1/\nu}. \tag{4.27}$$

Now, the lower bounds on rupture life will be given. In order to use the formulae (4.5) and (4.7), it is necessary to know the steady-state stress distribution σ^s_{ij}. This state is easy to obtain from the solutions (4.21)–(4.24) on putting there $\nu=n+1$. Thus for a constant load the expressions for the lower bound on rupture time and the representative rupture stress have the form

$$t_l=\left(\frac{n}{2P}\right)^{\nu}\frac{[1-(a/b)^{2/n}]^{\nu+1}}{A\,[1-(a/b)^{2(\nu+1)/n}]}, \tag{4.28}$$

$$\frac{\sigma_l}{P}=\frac{2}{n}\left\{\frac{1-(a/b)^{2(\nu+1)/n}}{(1+\nu)\,[1-(a/b)^{2/n}]^{\nu+1}}\right\}^{1/\nu}. \tag{4.29}$$

For cyclic loading we first find the steady-state cyclic stress distribution, $\sigma^{sc}_{ij}=\sigma^e_{ij}(t)+\rho_{ij}$. The linear elastic solution is given by

$$\sigma^e_r=-P(t)\frac{(b/r)^2-1}{(b/a)^2-1},\qquad \sigma^e_\varphi=P(t)\frac{(b/r)^2+1}{(b/a)^2-1},\qquad \sigma^e_z=\bar{\nu}\,(\sigma^e_r+\sigma^e_\varphi). \tag{4.30}$$

For the optimum lower bound we require a residual stress state ρ_{ij} which satisfies the equilibrium equation

$$\frac{d\rho_r}{dr}-\frac{\rho_\varphi-\rho_r}{r}=0 \tag{4.31}$$

and boundary conditions

$$\rho_r(a)=0,\qquad \rho_r(b)=0. \tag{4.32}$$

Further, the energy dissipated over a cycle will be minimized if the accumulated creep strains over the cycle due to $\sigma^{sc}_{ij}=\sigma^e_{ij}+\rho_{ij}$ are compatible, and therefore derivable from an increment of the radial displacement field $u(r)$. If we denote by v_r, v_φ, v_z the accumulated creep strains over a complete cycle, then from the condition $v_r+v_z+v_\varphi=0$. ($v_z=0$) and the relations $v_r=du/dr$, $v_\varphi=u/r$ we obtain a differential equation which has the solution

$$u=u(a)\,a/r, \tag{4.33}$$

where $u(a)$ is a constant to be determined. Assuming $\varphi=\sigma^{sc}_\varphi-\sigma^{sc}_r$, integrating Eqs. (2.3) for $\psi=1$ accounting for Eq. (4.32), we get

$$\frac{u(a)\,a}{r^2}=\int_0^T K(\sigma^e_\varphi-\sigma^e_r+\rho_\varphi-\rho_r)^n\,dt. \tag{4.34}$$

For the prescribed history of $P(t)$, Fig. 5 and Eqs. (4.30), Eq. (4.34) has the form

$$\frac{u(a)\,a}{KTr^2}=\mu\left[\frac{2P}{(b/a)^2-1}\left(\frac{b}{r}\right)^2+\rho_\varphi-\rho_r\right]^n+(1-\mu)\left[\frac{2\lambda P}{(b/a)^2-1}\left(\frac{b}{r}\right)^2+\rho_\varphi-\rho_r\right]^n. \tag{4.35}$$

To solve this equation for $\rho_\varphi-\rho_r$, we apply to the parenthetical expressions Newton's

The corresponding representative rupture stresses are: for a constant load, σ_u, for cyclic loading, $\sigma_u\,\gamma\,(t)$, where

$$\frac{\sigma_u}{p}=1/[(\gamma_1/\beta_1+1)\,(\gamma_1\,\beta_1^{1/(\nu-1)}+1)^{\nu-1}]^{1/\nu}. \tag{4.15}$$

Now, the lower bounds on rupture life will be given. Finding the steady state distribution σ_{ij}^s and inserting it into Eqs. (4.5) and (4.7), we obtain for the case of a constant load the following expressions for the lower bound on rupture time and the representative rupture stress:

$$t=\frac{(\gamma_1\,\beta_1^{1/n}+1)^{\nu+1}}{(1+\nu)\,Ap^{\nu}(\gamma_1\,\beta_1^{(\nu+1)/n}+1)}, \tag{4.16}$$

$$\frac{\sigma_l}{p}=\frac{(\gamma_1\,\beta_1^{(\nu+1)/n}+1)^{1/\nu}}{(\gamma_1\,\beta_1^{1/n}+1)^{(\nu+1)/\nu}}. \tag{4.17}$$

For the case of cylic loading it is necessary to know the cyclic steady-state stress distribution $\sigma_{ij}^{sc}(t)=\sigma_{ij}^e(t)+\rho_{ij}$. This state is found by choosing ρ to minimize the expression for the energy dissipation D over a cycle

$$\frac{D}{TA_2\,l_2\,p^{n+1}}=\mu\left[\frac{\gamma_1}{\beta_1}\left(\frac{\beta_1}{\gamma_1\,\beta_1+1}-\rho\right)^{n+1}+\left(\frac{1}{\gamma_1\,\beta_1+1}+\frac{\rho}{2}\right)^{n+1}\right]+ \tag{4.18}$$

$$+(1-\mu)\left[\frac{\gamma_1}{\beta_1}\left(\frac{\beta_1\,\lambda}{\gamma_1\,\beta_1+1}-\rho\right)^{n+1}+\left(\frac{\lambda}{\gamma_1\,\beta_1+1}+\frac{\rho}{2}\right)^{n+1}\right],$$

where $\rho=-\rho_1/p$ is a measure of the self-equilibrating stress field. On using this minimum value ρ and the expression (4.6), we arrive at the formula for the rupture time

$$t_l=\frac{\mu\left[\left(\frac{\beta_1}{\gamma_1\,\beta_1+1}-\rho\right)^{n+1}+\frac{\beta_1}{\gamma_1}\left(\frac{1}{\gamma_1\,\beta_1+1}+\frac{\rho}{2}\right)^{n+1}\right]+}{+(1-\mu)\left[\left(\frac{\lambda\beta_1}{\gamma_1\,\beta_1+1}-\rho\right)^{n+1}+\frac{\beta_1}{\gamma_1}\left(\frac{\lambda}{\gamma_1\,\beta_1+1}+\frac{\rho}{2}\right)^{n+1}\right]} \tag{4.19}$$

$$(1+\nu)\,Ap^{\nu}\left\{\mu\left[\left(\frac{\beta_1}{\gamma_1\,\beta_1+1}-\rho\right)^{n+1+\nu}+\frac{\beta_1}{\gamma_1}\left(\frac{1}{\gamma_1\,\beta_1+1}+\frac{\rho}{2}\right)^{n+1+\nu}\right]+\right.$$

$$\left.+(1-\mu)\left[\left(\frac{\lambda\beta_1}{\gamma_1\,\beta_1+1}-\rho\right)^{n+1+\nu}+\frac{\beta_1}{\gamma_1}\left(\frac{\lambda}{\gamma_1\,\beta_1+1}+\frac{\rho}{2}\right)^{n+1+\nu}\right]\right\}.$$

The corresponding representative rupture stress is $\sigma_l\,\gamma\,(t)$, where

$$\frac{\sigma_l}{p}=1/\{(1+\nu)\,Ap^{\nu}\,t_l\,[\mu+\lambda^{\nu}(1-\mu)]\}^{1/\nu}. \tag{4.20}$$

The above expressions are valid for the two-bar structure which operates at constant temperature. Data for the computations are given in Sect. 3.1 and the numerical results are presented in Table 5. It was found that the values $\rho=0.214$; 0.170; 0.135 minimized the energy dissipation, Eq. (4.18), for $\theta=500$; 550; 575°C, respectively.

formula for a binomial with arbitrary exponent which expresses an infinite series and retain only two terms. This series is absolutely converging if $|\rho|<\begin{cases}\beta\\ \lambda\beta\end{cases}$, where

$$\beta=\frac{2P}{(b/a)^2-1}\,\frac{b^2}{r^2},\qquad \rho=\rho_\varphi-\rho_r. \tag{4.36}$$

We get the following equation:

$$\frac{u(a)\,a}{KTr^2}\cong[\mu+(1-\mu)\,\lambda^n]\,\beta^n+n\,[\mu+(1-\mu)\,\lambda^{n-1}]\,\rho\beta^{n-1}, \tag{4.37}$$

from which we determine

$$\rho=\frac{u(a)\,a-KT\beta^n\,[\mu+(1-\mu)\,\lambda^n]\,r^2}{KTr^2\,n\,[\mu+(1-\mu)\,\lambda^{n-1}]\beta^{n-1}}. \tag{4.38}$$

Equations (4.31) and (4.32) yield the condition

$$\int_a^b\frac{\rho}{r}\,dr=0, \tag{4.39}$$

from which we calculate $u(a)$ and insert into Eq. (4.38). We thus obtain

$$\rho_\varphi-\rho_r=\frac{2P\,[\mu+(1-\mu)\,\lambda^n]}{n\,[\mu+(1-\mu)\,\lambda^{n-1}]}\left[\frac{(n-2)\,(r/b)^{2(n-2)}}{1-(a/b)^{2(n-2)}}-\frac{(b/r)^2}{(b/a)^2-1}\right]. \tag{4.40}$$

Now, the condition for convergence of the considered series was checked numerically to be satisfied throughout the thickness of the tube. Using again Eqs. (4.31) and (4.32) we finally get the following expressions for the components of the residual stress-state:

$$\rho_r=\int_a^r\frac{\rho}{r}\,dr=\frac{P\,[\mu+(1-\mu)\,\lambda^n]}{n\,[\mu+(1-\mu)\,\lambda^{n-1}]}\left[\frac{(r/a)^{2(n-2)}-1}{(b/a)^{2(n-2)}-1}-\frac{(a/r)^2-1}{(a/b)^2-1}\right], \tag{4.41}$$

$$\rho_\varphi=\frac{P\,[\mu+(1-\mu)\,\lambda^n]}{n\,[\mu+(1-\mu)\,\lambda^{n-1}]}\left[\frac{(2n-3)\,(r/a)^{2(n-2)}-1)}{(b/a)^{2(n-2)}-1}+\frac{(a/r)^2+1}{(a-b)^2-1}\right], \tag{4.42}$$

which, together with Eqs. (4.30), determine the stress distribution σ_{ij}^{sc}. The functions u i φ have the form

$$u=\frac{(2P)^n\,TKb^2\,(n-2)\,[\mu+(1-\mu)\,\lambda^n]}{r\,[(b/a)^2-1]^{n-1}\,[1-(a/b)^{2(n-2)}]}, \tag{4.43}$$

$$\varphi=\frac{2P(t)}{(b/a)^2-1}\left(\frac{b}{r}\right)^2+\frac{2P\,[\mu+(1-\mu)\,\lambda^n]}{n\,[\mu+(1-\mu)\,\lambda^{n-1}]}\left[\frac{(n-2)\,(r/b)^{2(n-2)}}{1-(a/b)^{2(n-2)}}-\frac{(b/r)^2}{(b/a)^2-1}\right]. \tag{4.44}$$

Having determined the function φ, Eq. (4.44), the formulae (4.6) and (4.8) for the lower bound on the rupture time t_l and the representative rupture stress $\sigma_l\,\gamma\,(t)$ have the form

$$t_l = \frac{\int_a^b \int_0^1 \varphi^{n+1}\, r dx dr}{(1+\nu) A \int_a^b \left(\int_0^1 \varphi^{n+1}\, dx \int_0^1 \varphi^{\nu}\, dx \right) r dr}, \tag{4.45}$$

$$\frac{\sigma_l}{P} = \left\{ \frac{\int_a^b \left(\int_0^1 \varphi^{n+1}\, dx \int_0^1 \varphi^{\nu}\, dx \right) r dr}{P^{\nu}[\mu + \lambda^{\nu}(1-\mu)] \int_a^b \int_0^1 \varphi^{n+1}\, r dx dr} \right\}^{1/\nu}. \tag{4.46}$$

In general, the exponents in Eqs. (4.45) and (4.46) are not integers, so according to Chebyshev's theorem they cannot be expressed by means of elementary functions. Therefore, as earlier, the expressions under the integrals were expanded into series using Newton's formula for a binomial and three terms were retained. Further ntegration and checking of the convergence condition of the series were performed numerically. The computed values for the data given in Sect. 3.2 are listed in Table 6 .

Table 6. Thick cylinder. Bounds on rupture time and representative rupture stresses

Temperature	Constant load		Cyclic loading	
	Lower bound (4.28), (4.29)	Upper bound (4.25), (4.27)	Lower bound (4.44), (4.45)	Upper bound (4.26), (4.27)
500°C	$t_l = 22.4312 \cdot 10^4$ $N = 9346$ $\sigma_l/P = 2.49045$	$t_u = 24.0340 \cdot 10^4$ $N = 1014$ $\sigma_u/P = 2.42657$	$t_l = 32.4631 \cdot 10^4$ $N = 13526$ $\sigma_l/P = 2.48476$	$t_u = 34.5679 \cdot 10^4$ $N = 14403$ $\sigma_u/P = 2.42657$
550°C	$t_l = 1.3617 \cdot 10^4$ $N = 567$ $\sigma_l/P = 2.50251$	$t_u = 1.4811 \cdot 10^4$ $N = 617$ $\sigma_u = /P = 2.39729$	$t_l = 1.9007 \cdot 10^4$ $N = 792$ $\sigma_l/P = 2.49258$	$t_u = 2.0515 \cdot 10^4$ $N = 855$ $\sigma_u/P = 2.39729$
575°C	$t_l = 0.5895 \cdot 10^4$ $N = 246$ $\sigma_l/P = 2.51889$	$t_u = 0.6506 \cdot 10^4$ $N = 271$ $\sigma_u/P = 2.38674$	$t_l = 0.8116 \cdot 10^4$ $N = 338$ $\sigma_l/P = 2.51397$	$t_u = 0.8925 \cdot 10^4$ $N = 372$ $\sigma_u/P = 2.38674$

$P = 310$ KG/cm^2, $\lambda = 0.4$, $\mu = 2/3$, $T = 24$ hrs, $b/a = 1.5$, $t_{l,u}$ — [hr], N — Number of days or cycles

6. Conclusions

The aim of this paper was to show the possibilities of a useful description of the creep behaviour of material at elevated constant and variable temperature and under proportional cyclic loading. Thus, only such functions are introduced into the constitutive equations which may be determined from the results of technically possible experiments in the uni-axial stress state, i.e. n and K from the creep curve for the steady state conditions, A and ν from the rupture curve. The theoretical curves obtain-

ed from Eqs. (2.9) and (2.11) coincide with the experimental results for the investigated steel BS 1501–271 in the temperature range from 500°C to 575°C (Figs. 1 and 2). Also, a comparison of the values of strains to rupture for the two-bar structure, Table 3, with these given in Table 2 confirms the suitability of the description. Particular analysis of numerically computed strains in a cycle has shown that after each step down the loading and temperature the strain is initially constant or insignificantly decreases but after that, the strain begins to be on the slow increase. This depends on the value of a jump and an advanced crepp process. Next, after a step up of loading and temperature, an acceleration of creep occurred. These phenomena are observed in the experiments. In Figs. 6 (the two-bar structure) and 9 (the thick cylinder, v_{φ}, u assign the values over the cycle) the significant acceleration of the creep process can be noticed when the time approaches the time to rupture. In Fig. 9 the stress redistribution and the propagation of the damage front are shown for the case of constant pressure and constant temperature. In Figs. 11, 12 and 13 the stress redistribution for the case of constant pressure and a constant or cyclic temperature gradient is presented. The stress redistribution is particularly visible in Fig. 8 where the significant influence of non-isothermal conditions on the stress distribution for steady state is also shown.

Depending on the temperature gradient, the value or pressure and the dimensions of the cylinder, the first rupture can appear at $r \geqslant a$. For example, in some cases the values $r/a = 1.05 \div 1.085$ were obtained for the first rupture, Table 4.

The experimental results [16] and the numerical results for the structures show a significant influence of the elevated temperature and its fluctuations on the failure time. For the two-bar structure under a constant load and the temperature 550°C we get the rupture time 25 times shorter and at the temperature 575°C 64 times shorter than for the temperature 500°C. Similar results are obtained for cyclic changes of temperature. For example, for a constant load cyclic changes in the range 500–550°C shorten the rupture life 13.5 times and cyclic changes in the range 500–575°C to 33 times in comparison with the result for a constant temperature of 500°C. Table 3. For a thick cylinder subjected to constant pressure the following results are obtained, for example: for a constant temperature $\theta(a) = \theta(b) = 575°C$ the time to the first rupture is about 5 times shorter than at $\theta(a) = 575°C - \theta(b) = 500°C$. For a constant gradient $\Delta\theta = 75°C$ $[\theta(a) = 575°C - \theta(b) = 500°C]$ the time to the first rupture is 1.6 times shorter in comparison with the result for $\Delta\theta = 50°C$ $[\theta(a) = 550°C - \theta(b) = 500°C]$ and 1.4 times shorter than for the case of a cyclic temperature gradient $\Delta\theta = 75°C$ $[\theta(a) = 575°C - \theta(b) = 500°C]$, Fig. 5. In the case of a constant temperature gradient $\Delta\theta = 75°C$ $[\theta(a) = 575°C - \theta(b) = 500°C]$, the time to the first rupture for the proportional cyclic pressure is about 1.4 times longer as compared with the time for constant pressure, Table 4.

The cyclic change of temperature causes the strains to rupture to increase in comparison with corresponding values for constant lower temperature in a cycle. However, for constant temperature the cyclic proportional changes of loading diminish the strains to rupture as compared to the values for constant lower loading in a cycle, Tables 3 and 4.

The methods for bounding the rupture life used in this paper are valid for the structures which operate at constant tempratures. For the two-bar structure subjected to a constant load the lower bounds differ from the exact values from 0.7% to 4% and the upper bounds from 14% to 17.6%. However, for cyclic loading the lower estimates differ considerably from the exact solution, namely from 67% to 53% (it is so far the worst result obtained for this structure) and the upper estimates from 17.4% to 19%, for the temperature range 500–575°C, Tables 3 and 5. For a thick cylinder under constant temperature the exact solution was calculated only for $\theta(a) = \theta(b) = 575$°C. The lower bounds differ from this exact result less than 1% and the upper bounds about 9%, for both cases of loading, constant and cyclic, Tables 4 and 6. It can be seen from Tables 4 and 6 that the obtained estimates of rupture life are precise enough for design purposes (except perhaps for the two-bar structure under cyclic loading). It is worth mentioning that all bounds were computed by means of a pocket calculator, while for the exact solution it was necessary to use a CDC computer.

In this work the effects of high temperature fatigue are ignored. This can be justified by the fact that the maximum operating stress levels are small fractions of the yield stress and for the cycle periods selected the material deformations are predominantly that of creep. The cases of the structures under combined loadings are considered in the papers PIECHNIK and CHRZANOWSKI [22], ŻYCZKOWSKI and SKRZYPEK [23].

Concluding, the obtained results clearly show the substantial influence of elevated temperature, temperature gradients, its cyclic flucutuations and cyclic proportional loading upon the stress redistribution, the magnitude of deformation, the propagation of the damage front and the rupture life.

The introduced description of the creep rupture behaviour of a material and the methods for bounding the rupture life of structures indicate the possibilities of solutions to the practical problems encountered, for example in structural mechanics of reactor technology.

REFERENCES

1. A. K. PENNY and D. L. MARRIOTT, *Design for creep*, McGraw-Hill Book Company (UK) Limited, London 1971.
2. I. A. ODING, V. S. IVANOVA, V. V. BURDUKSKII and V. N. GEMINOV, *Creep and stresses relaxation in metals* (in English), Oliver and Boyd, London 1965.
3. A. J. KENNEDY, *Processes of creep and fatigue in metals*, Oliver and Boyd, London 1962.
4. S. TAIRA, *Lifetime of structures subjected to varying load and temperature*, Creep in Structures, IUTAM Colloquium, (Stanford 1960), Proc. N. J. Hoff, Springer-Verlag, Berlin 1962.
5. L. H. TOFT and T. BROON, *Exploratory tests on the effects of temperature and load cycling on the creep resistance and micro-structure of two oustentic steels*, Joint Inter. Conf. on Creep, New York, London 1963, Proc. 178, 3A, 1963–64.
6. G. P. TILLY, *Estimation of creep and fatigue under cycling loading*, J. Strain Anal., 7, 4, 1972.
7. V. S. NAMESTNIKOV, *Forward and reverse torsion under creep conditions*, PMTF, 1., 1960.

8. J. MORROW and G. R. HALFORD, *Creep under repeated stress reversals*, Joint Inter. Conf. on Creep, New York, London 1963, Proc. 178, 3A, 1863–64.

9. D. R. HAYHURST, *Estimates of the creep rupture life of structures subjected to variable loading*, Univ. Leicester, Dept. Engng., Report 74 — 13.

10. Yu. N. RABOTNOV, *Creep problems in structural members* (in English), North-Holland, Amsterdam 1969.

11. A. R. S. PONTER, *Deformation , displacement and work bounds for structures in a state of creep and subjected to variable loading*, ASME, 72 — APM — U.

12. F. K. G. ODQVIST and J. HULT, *Kriechfestigkeit metallischer Werkstoffe*, Springer-Verlag, Berlin 1962.

13. L. M. KACHANOV, *Theory of creep* (in English), National Lending Library, Boston Spa 1967.

14. F. A. LECKIE and D. R. HAYHURST, *Creep rupture of structures*, Proc. Roy. Soc., A340, 323, London 1974.

15. V. P. SDOBYREV, *Criteria of ultimate strength for various heat-treated alloys in intricate states of stress*, Academy of Sciences, OTN, Mechanics and Mechanical Engineering, 6, 1959 (in Russian).

16. J. GLEN and L. K. HAZRA, *Some information of creep behaviour of low alloy steels*, Proc. Symp. Presentation of creep strain data, October 1971, Corporate Lab. BSC, London 1972.

17. W. WOJEWÓDZKI, *Creep rupture of structures subjected to variable loading and temperature*, Trans. 3rd Int. Conf. Struct. Mech. in Reactor Tech., Paper L5/70, London 1975.

18. L. M. KACHANOV, *Rupture time under creep conditions*, Problems of Continuum Mechanics, Izd. AN SSSR, Moscow 1961 (in Russian).

19. F. A. LECKIE and W. WOJEWÓDZKI, *Estimates of rupture life-constant load*, Int. J. Solids Struct., **11**, 1357–1365, 1975.

20. F. A. LECKIE and W. WOJEWÓDZKI, *Estimates of the rupture life of structural components subjected to proportional cyclic loading*, J. Mech. Phys. Solids, 24, 239–250, 1976.

21. A. R. S. PONTER, *On the stress analysis of creeping structures subjected to variable loading*, J. Appl. Mech., **40**, 589, 1973.

22. S. PIECHNIK and M. CHRZANOWSKI, *Time of total creep rupture of a beam under combined load*, Second IUTAM Symp. of Creep in Structures, (Göteborg 1970), Proc. J. Hult ed., Springer-Verlag, Berlin 1972.

23. M. ŻYCZKOWSKI and J. SKRZYPEK, *Stationary creep and creep rupture of a thick-walled tube under combined loadings*, Second IUTAM Symp. of Creep in Structures, (Göteborg 1970), Proc., J. Hult ed., Springer-Verlag, Berlin 1972.

STRESZCZENIE

ZNISZCZENIE PEŁZAJĄCE KONSTRUKCJI W PODWYŻSZONYCH TEMPERATURACH I OSZACOWANIE CZASU ZNISZCZENIA

Zaproponowano opis zniszczenia pełzającego w podwyższonej temperaturze. Funkcje występujące w równaniach konstytutywnych określono na podstawie możliwych technicznie do przeprowadzenia doświadczeń w jednoosiowym stanie naprężenia. Wykazano, że zaproponowany opis jest wygodny do badania wpływu podwyższonej temperatury, gradientów temperatury, jej cyklicznych fluktuacji i cyklicznego proporcjonalnego obciążenia na rozkład naprężenia, wielkość odkształcenia, propagację frontu pęknięcia i czas zniszczenia konstrukcji. Wykorzystując metody oszacowania czasu zniszczenia konstrukcji, otrzymano również dolne i górne oszacowanie dla prostych konstrukcji i porównano je z podanymi rozwiązaniami ścisłymi.

Р е з ю м е

ПОЛЗУЧЕСТЬ КОНСТРУКЦИЙ В ПОВЫШЕННОЙ ТЕМПЕРАТУРЕ ПРИВОДЯЩАЯ К РАЗРУШЕНИЮ И ОЦЕНКА ВРЕМЕНИ ДО РАЗРУШЕНИЯ

В статье дается описание ползучести приводящей к разрушению в условиях повышенной температуры. Функции введенные в уравнения состояния определены из результатов технически возможных экспериментов в одноосном напряженном состоянии. Показано, что применяя описание, можно исследовать влияние повышенной температуры, градиентов температуры и их циклических изменений, а также влияние пропорциональной циклической нагрузки на изменение напряжений, величину деформаций, распространение фронта разрушения и времени до разрушения конструкции. Использованы также методы определения пределов времени до разрушения конструкции, определены для простых конструкций нижные и верхние пределы и сравнены с данным точным решением.

TECHNICAL UNIVERSITY OF WARSAW

Received April 27, 1977.